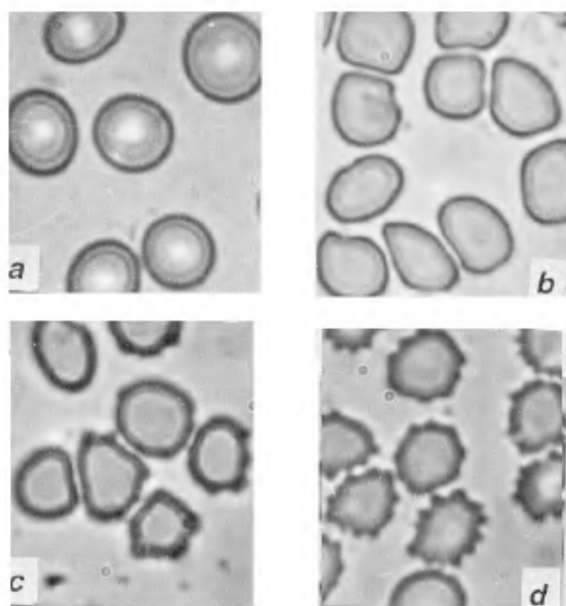


multiplying with pixel area, the area ( $A$ ) of the cell was determined. Similarly, by counting the number of pixels along the perimeter and then multiplying with pixel length, the perimeter ( $P$ ) of the same cell was determined.

Based on these, the form factor ( $FF$ ) =  $P^2/4\pi A$  was calculated. This parameter is the measure of compactness or roundness of the cell and its variation indicates the deviation of the shape in the image from that of a disc ( $FF$  for disc = 1). The calibration of the above measurement procedure was carried out by determining area and perimeter of a circle of known diameter. This procedure was further verified with similar measurement of circles of known diameters. A good agreement between the measured and calculated values was obtained. Statistical analysis of the data was carried out by Student's  $t$ -test.

Figure 2 shows the images of the erythrocytes, normal and after incubation for half, one and two hours, as obtained by phase contrast microscope. The gradual changes in normal erythrocytes during cholesterol-enrichment up to two hours are clearly observed. Figure 3 shows the contour of the erythrocytes as obtained from



**Figure 2.** Images of erythrocytes as obtained by phase contrast microscope. *a*, normal; and after incubation in cholesterol-enriched plasma for *b*,  $\frac{1}{2}$  h; *c*, 1 h; and *d*, 2 h.

the sequence of images by image processing procedures. A transition from discocytes to crenated erythrocytes as obtained by this process is attributed to cholesterol accumulation in the middle layer of the membrane<sup>9</sup>. Deviation from the discoid shape after half an hour shows the accumulation of cholesterol in the membrane. Further accumulation leads to distortion of the shape and finally crenation of the erythrocytes<sup>10</sup>. This alteration also results in change in the brightness of the central pallor, indicating that there is gradual transition from discocytes to acanthocytes/echinocytes<sup>26</sup>.

The shape parameters (Table 1) show the respective variations. The area shows highly significant decrease with the increase of C/P of the erythrocyte membrane. In contrast to this, the perimeter shows a highly significant increase with the change in shape in erythrocytes. The crenated cells, after incubation for 2 h show minimum area and maximum perimeter compared to normal cells.

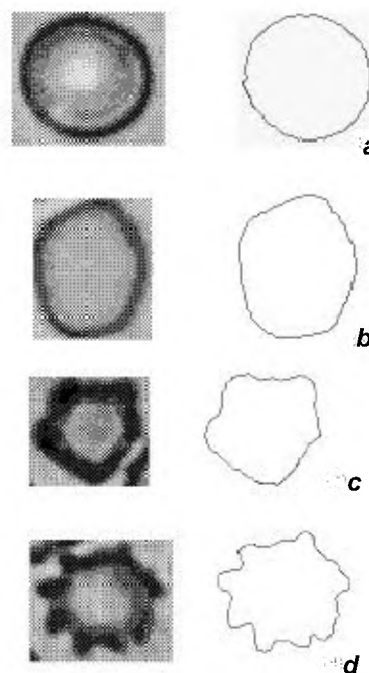


**Figure 3.** Shape and contours of erythrocytes. *a*, normal; and after incubation for *b*,  $\frac{1}{2}$  h; *c*, 1 h; and *d*, 2 h.

**Table 1.** Shape parameters of normal and cholesterol-enriched erythrocytes after incubation in cholesterol-enriched plasma for  $\frac{1}{2}$ , 1 and 2 hours

| Shape parameter          | Erythrocytes         |                    |                    |                    |
|--------------------------|----------------------|--------------------|--------------------|--------------------|
|                          | After incubation for |                    |                    |                    |
|                          | Normal               | $\frac{1}{2}$ hour | 1 hour             | 2 hour             |
| Area, $\mu\text{m}^2$    | $51.17 \pm 0.35^+$   | $49.92 \pm 0.7^*$  | $47.85 \pm 0.41^*$ | $46.85 \pm 0.7^*$  |
| Perimeter, $\mu\text{m}$ | $25.5 \pm 0.35^+$    | $28.75 \pm 0.47^*$ | $29.93 \pm 0.69^*$ | $32 \pm 1.44^*$    |
| Form factor              | $1.011 \pm 0.02^+$   | $1.31 \pm 0.02^*$  | $1.48 \pm 0.09^*$  | $1.738 \pm 0.23^*$ |

+, Mean  $\pm$  SD, \*,  $P < 0.0005$ .

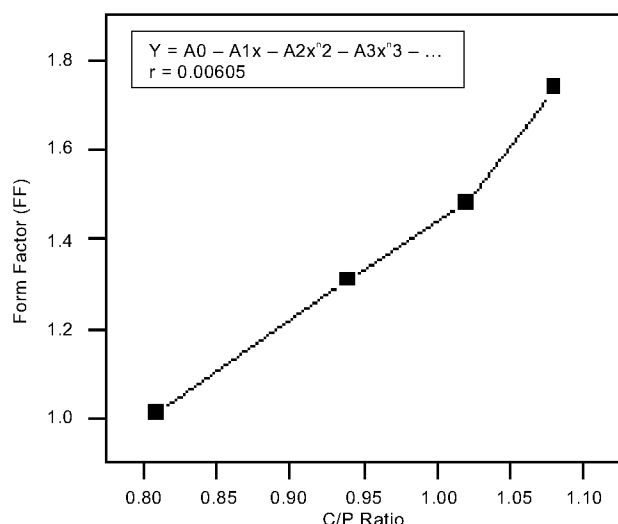


Figure 4. Variation of the FF of erythrocytes at various C/P ratios.

The FF increases significantly for erythrocytes incubated for various intervals. The discoid shape of normal cells is close to that of the disc, whereas all other shapes show significant deviations. Figure 4 shows the variation of the FF and C/P ratio at various incubation intervals, indicating that changes in the FF may correspond to respective changes in plasma composition. This also shows that the cholesterol uptake by erythrocytes is a fast process, which is attributed to its neutral electrical properties.

The present studies show that the morphological changes as described by these parameters are correlated with the C/P ratio of erythrocytes ( $r = 0.99605$ ), determinant of *in vivo* hypercholesterolemic conditions. But the extent of changes during this process in the vascular system could not be predicted based on these observations. Further studies on laboratory animals are required to correlate these parameters. Other parameters such as elongation, major and minor axes lengths, and roughness of erythrocyte, as calculated in patients with coronary artery disease<sup>19</sup>, can further be applied in highlighting the changes induced in the cells in various diseases.

1. Bessis, M., Weed, R. I. and Leblond, P. F., *Red Cell Shape*, Springer-Verlag, Berlin 1973.
2. Marchesi, V. T., *Blood*, 1983, **61**, 1–11.
3. Lowe, G. D. O., *Clinical Blood Rheology*, CRC Press, Boca Raton, 1988, vol. 1.
4. Chien, S., Dormandy, J., Ernst, E. and Matrai, *Clinical Hemorheology*, M. Nijhoff, Boston, 1987.
5. Stoltz, J. F., Singh, M. and Riha, P., *Hemorheology in Practice*, IOS Press, Amsterdam, 1999.
6. Weed, R. I., La Celle, P. L. and Merrill, E. W., *J. Clin. Invest.*, 1969, **48**, 795–809.
7. Crum, L. A., Coakley, W. T. and Deeley, J. O. T., *Biochem. Biophys. Acta*, 1979, **554**, 76–89.
8. Ramakrishnan, S., Grebe, R., Singh, M. and Schmid-Schonbein, H., *Curr. Sci.*, 1994, **77**, 805–808.

9. Nagaprasad, V. and Singh, M., *Clin. Hemorheol.*, 1998, **18**, 273–284.
10. Vaya, A., Martinez, M., Sloves, P., Barbera, J. L. and Aznar, J., *Clin. Hemorheol.*, 1996, **16**, 515–522.
11. Vatsala, T. M. and Singh, M., *Atherosclerosis*, 1980, **36**, 39–45.
12. Kanakaraj, P. and Singh, M., *Atherosclerosis*, 1989, **76**, 209–217.
13. Vassala, T. M. and Singh, M., *Curr. Sci.*, 1979, **48**, 797–799.
14. Abugo, O. O., Peddada, R. R., Kelly, J. F., Roth, G. S. and Riftind, J. M., *Clin. Hemorheol.*, 1997, **17**, 437–443.
15. Singh, M. and Kanakaraj, P., *Indian J. Exp. Biol.*, 1985, **23**, 454–459.
16. Kanakaraj, P. and Singh, M., *Indian J. Biochem. Biophys.*, 1989, **26**, 381–385.
17. Vatsala, T. M. and Singh, M., *Artery*, 1980, **7**, 519–530.
18. Jones, G. T. and Stehbins, W. E., *Pathology*, 1995, **27**, 333–338.
19. Alexandratou, E., Yova, D. and Cokkinos, D. V., *Clin. Hemorheol. Microcirc.*, 1999, **21**, 181–188.
20. Chen, S., Gavish, B., Zhang, S., Mahler, Y. and Yedgar, S., *Biorheology*, 1995, **32**, 487–496.
21. Baginski, E. S. and Zak, B., *Gradwhl's Clinical Laboratory Methods and Diagnosis* (eds Frankel, S., Reitman, S. and Sommerwirth, A. C.), C. V. Mosby Co., St. Louis, 1970, p. 236.
22. Naito, H. K., *Clin. Chem.*, 1975, **21**, 1454.
23. Gonzalez, R. C. and Woods, R. E., *Digital Image Processing*, Addison-Wesley, Readings, 1993.
24. Rosenfield, A. and Kak, A. C., *Digital Picture Processing*, Academic Press, New York, 1982, vol. 1.
25. Zampieri, P., *Pattern Recognition*, 1963, **15**, 161.
26. Bessis, M., in *Red Cell Shape* (eds Bessis, M., Weed, R. I. and Leblond, P. F.), Springer-Verlag, Berlin, 1973, pp. 1–25.

Received 27 March 2000; revised accepted 6 October 2000

## Resistance of P-solubilizing *Acetobacter diazotrophicus* to antibiotics

Sarita Mowade and P. Bhattacharyya\*

Regional Biofertilizer Development Centre, N.S. Building, Civil lines, Nagpur 440 001, India

**A local isolate (Nagpur) of *Acetobacter diazotrophicus* having the capacity to solubilize insoluble phosphate in Pikovskaya's medium and Sperber's medium was tested for its response to different antibiotics under *in vitro* condition. The isolate was found to be resistant to ampicillin, erythromycin and roxithromycin even at higher concentrations and less sensitive to penicillin and tetracycline. The sensitivity of the bacterium was observed more with antibiotics like ciprofloxacin, doxycycline, rifampicin and chloramphenicol.**

THE role of *Acetobacter diazotrophicus* as nitrogen fixer<sup>1,2</sup> is well established. The endophytic bacterium con-

\*For correspondence.

tions, i.e. from 40 to 200 µg with the inhibition zones of 1.75, 1.5, 1.1, 1.75 and 2.6 cm, respectively.

These results were further confirmed by assessing the effect of different concentrations of various antibiotics on total viable population of test bacterium as reported in Table 2. The growth response of the organism to antibiotics against each concentration has been represented in Figure 2. Data presented here show that the growth of the organism was not affected by erythromycin, ampicillin, roxythromycin. The population showed the declining growth pattern in penicillin and tetracycline-incorporated plates from 120 µg and 160 µg, respectively. Whereas the population of the bacterium was negligible in plates incorporated with antibiotics like ciprofloxacin, chloramphenicol, doxycyclin, streptomycin and rifampicin even at the lowest concentration of 40 µg.

These observations clearly indicate that this particular isolate was resistant to erythromycin, ampicillin, and roxithromycin then to penicillin and tetracycline. And the same was sensitive to ciprofloxacin, doxycyclin, rifampicin, chloramphenicol and streptomycin sustaining earlier reports in a study with *Rhizobium*<sup>11</sup>.

These properties can be used as a stable marker for identifying the P-solubilizing strain of *A. diazotrophicus*, where the strain should be screened for resistance against erythromycin, ampicillin, and roxithromycin at 200 µg/ml concentration.

1. Reis, V. M. *et al.*, *World J. Microbiol. Biotechnol.*, 1994, **10**, 401–405.
2. Boddey, Robert M., *Crit. Rev. Plant Sci.*, 1995, **14**, 263–279.
3. Bhattacharyya, P. *et al.*, Souvenir, North Eastern, Regional Conference on Biofertilizer, 22–23, January, 1999.
4. Maheshkumar, K. S. *et al.*, *Cur. Sci.*, 1999, **76**, 874–875.
5. Moawad, H. and Bohlool, B. B., *World J. Microbiol. Biotechnol.*, 1992, **8**, 387–392.
6. Cavalcante Vladamir, A. and Dobereiner, J., *Plant Soil*, 1998, **108**, 23–31.
7. Banik, S. and Dey, B. K., *Microbiology*, 1983, **138**, 17–23.
8. Waksman, S. A. and Reilly, H. C., *Ind. Eng. Chem. Anal. Edn.*, 1945, **17**, 556–558.
9. Chakravorty, B. P. and Rangarajan, M., *Hindustan Antibiotic Bull.*, 1966, **8**, 209–211.
10. Kingley, M. T. and Bohlool, B. B., *Can. Microbiol.*, 1983, **29**, 518–526.
11. Schiwinghamer, E. A., *Antonie van Leeuwenhoek*, 1967, **33**, 12–136.
12. Pikovskaya, R. I., *Mikrobiologiya*, 1948, **17**, 362–370.

Received 8 May 2000; revised accepted 7 September 2000

## K-feldspar metasomatism in granulite-facies rocks of Palghat region, Kerala: Evidence and implications of brines in charnockite-forming metamorphism

Subhash Sukumaran and G. R. Ravindra Kumar\*

Centre for Earth Science Studies, Akkulam,  
Thiruvananthapuram 695 031, India

Formation of granulites requires low H<sub>2</sub>O activity and fluids play a major role in their evolution. A wide variety of granulite-forming processes have been discussed in the literature. Among the models proposed, the presence of fluid inclusions, alkali metasomatism and loss of large ion lithophile (LIL) elements support the fluid-driven granulite-forming process. In this paper we document abundant petrographic evidence in the Palghat region for the alkali metasomatism and evidence for metamorphic fluid of low aH<sub>2</sub>O in rocks like banded charnockite, hornblende–biotite gneiss and incipient charnockite. Evidence of potash metasomatism is noted as (a) rims of K-feldspar along orthopyroxene, opaque, plagioclase and K-feldspar grains, (b) veins of secondary K-feldspars traversing plagioclase and hornblende and (c) in the form of blebs in plagioclase grains and as exsolution. Excellent evidence of K-feldspar veins growing along the borders of orthopyroxene grains indicates that the vein network represents deposition of migrating XH<sub>2</sub>O halide-rich fluids. These low H<sub>2</sub>O brines may have created a conducive environment for localized breakdown of biotite and development of incipient charnockite.

THE role of fluids in the process of metamorphic recrystallization is well recognized in many of the metamorphic terrains and has since received special emphasis in the metamorphic transformation of gneiss to charnockite<sup>1</sup>. Although opinions are divided as to the source of fluids, existence of large amounts of carbon dioxide-rich fluids is recorded in almost all cases of charnockite development. The essential role of fluids is particularly evident in small mixed gneiss-charnockite quarries of southern India. Recently, there are interesting debates on the concentrated low activity brines as causative agents of granulite-facies metamorphism<sup>2–5</sup>. The new models propose that underplated basalts with alkaline affinities give off supercritical fluids rich in halides (Cl, F), H<sub>2</sub>O and CO<sub>2</sub> while passing through the lower crust. Because of the low wetting ability of CO<sub>2</sub> with quartz, CO<sub>2</sub> gets entrapped and helps in converting the lower crust to charnockites/granulites. This observation has acquired significance as the recent experimental work in the system NaCl–KCl–H<sub>2</sub>O at deep crustal temperature and pressure has demonstrated that

\*For correspondence. (e-mail: grrkumar@md4.vsnl.net.in)

concentrated brines have necessary low water activity, high alkali mobility and high infiltration ability<sup>6,7</sup>. These studies have therefore indicated brines as feasible granulite-facies fluids.

In the southern granulite terrain, especially in Palghat region, two types of charnockite, namely banded charnockite and incipient charnockite belonging to two different periods are noted. Banded charnockites (regional granulite) are recognized as the earliest, deep crustal product while arrested charnockites evolved later, perhaps during uplift. It is known that rocks undergo long and complex fluid-rock interaction during their ascent. The role of fluids, especially on the brines and accompanying changes in the post-peak metamorphic history is less studied because they have a very low tendency to be captured as fluid inclusions<sup>8</sup>. In this context we have examined a large number of samples from the Palghat region. We recognize K-feldspar veins enveloping orthopyroxene, and along the margins of plagioclase, similar to the observations made from other major high-grade terrains<sup>3,4,9</sup>. In this paper we illustrate several instances of K-feldspar veining and examine the role of alkali-rich fluids in the evolution of charnockites in the Palghat region.

The Palghat region in central Kerala is a part of the granulite belt of south India. The region is considered to mark a zone of contact between the northern Archaean block and dominantly Proterozoic block to the south (Pandyan Mobile Belt<sup>10</sup>). Major rock types in the region include, in order of abundance, hornblende-biotite gneiss, biotite gneiss, charnockite (regional granulite), amphibolite, granite and pegmatite. Occurrence of incipient charnockite overprinting hornblende-biotite gneisses has been reported recently<sup>11,12</sup>. Three deformation phases are recognized as F<sub>1</sub>, rootless isoclinal folds within the compositional bands of gneisses and amphibolites; F<sub>2</sub>, folds occurring as isoclinal to tight folds along EW; and F<sub>3</sub>, folds as warps with gentle plunges. Ages of rocks and metamorphism are poorly constrained. Recent K-Ar dates of mica in pegmatites, which cross-cut the gneisses, have yielded ages ~ 500 m.y.<sup>13</sup>.

All the major rock types like hornblende-biotite gneiss with enclaves of amphibolite and pyroxene granulite bodies, banded charnockite and biotite gneiss show evidence of extensive migmatization and deformation. Late coarse-grained pink quartzo-feldspathic pegmatites intrude all the rock types. Field relations indicate that the banded charnockite and grey hornblende-biotite gneiss are the earliest units as they are co-folded, co-planar and show imprints of similar deformation and migmatization<sup>11,12</sup>. Banded charnockites are extensive on a regional scale but on outcrop scale they may be noted as patches when pink quartzo-feldspathic pegmatite veins retrogress them at immediate contacts. Mafic minerals such as clinopyroxene, orthopyroxene, hornblende and biotite define the foliation. The banded charnockites are granoblastic with

an equigranular to inequigranular texture. Patches of unretrogressed, banded charnockites in grey retrogressed gneiss show continuation of foliation and similarity of grain sizes when traced into the gneiss. The incipient charnockites on the other hand, occur as small isolated patches or veins with granoblastic texture and grain size coarser than the surrounding gneiss. They are also characterized by lack of foliation and low concentration of mafic minerals. Structural control in the formation of incipient charnockite is evident in the field as they are always associated to foliation planes or foliation boudins or axial planes or shear zones. They are also seen at places as margins to biotite-rich dykes. It is observed that incipient charnockites are localized in the migmatitic hornblende-biotite gneiss, particularly to leucosomes or modified palaeosomes and are absent within pink granitic-biotite gneiss.

Micro-textural aspects commonly observed are a dominant granoblastic texture with effects of shearing under high ductility. Prograde textures of biotite + quartz => orthopyroxene + K-feldspar + fluid are observed in the transformation of hornblende biotite gneiss to incipient charnockite. The biotite grains involved in the biotite + quartz reaction show exsolution of opaque grains and in the charnockite portion these opaque exsolution accumulate to form large grains of hemo-ilmenite. The most interesting aspect is the recognition of late K-feldspar veining textures observed in the banded charnockite, hornblende-biotite gneiss and incipient charnockite. Textural studies document K-metasomatism as (a) rims of K-feldspar (Figure 1 a) along orthopyroxene (Figure 1 b), clinopyroxene, opaque (Figure 1 c) and microcline, (b) veins of secondary K-feldspar in larger plagioclase, orthopyroxene, hornblende and quartz grains (Figure 1 d).

Vein type K-metasomatism is the most common form and is traced along weak planes like sutures and cleavage planes. The vein types in some cases tend to increase the size of blebs within the perthite grain (Figure 2). Detailed studies of such textures are also reported by Safonov *et al.*<sup>14</sup> on incipient charnockite formation of Kurunegala, Sri Lanka. Sometimes they exhibit more than one generation as they show cross cutting relationship (Figure 3). This could indicate that K-metasomatism could have occurred over a long period. In some cases it is observed that these K-rich fluids have formed into larger secondary K-feldspar grains. In cases where patches invading plagioclase grains are seen, the polysynthetic twin lamellae are obliterated and patches of K-feldspar of irregular shapes are formed within larger plagioclase (Figure 4). This type of potash metasomatism is commonly observed in banded charnockite. It is also noted against orthopyroxene (Figure 5), clinopyroxene and perthites.

The effect of K-metasomatism is most pronounced and intensive in pink granites and pegmatites. Perthite grains rimmed by K-feldspar are also documented. This texture indicates that the granite was less viscous, enriched in